



Cite this: *RSC Adv.*, 2016, 6, 4792

Vanadium(v) phenolate complexes for ring opening homo- and co-polymerisation of ϵ -caprolactone, L-lactide and rac-lactide†

Feijie Ge,^a Yi Dan,^a Yahya Al-Khafaji,^b Timothy J. Prior,^b Long Jiang,^{*a} Mark R. J. Elsegood^c and Carl Redshaw^{*b}

The vanadyl complexes [VO(O*t*Bu)L¹] (**1**) and {[VO(O*i*Pr)]₂(μ -*p*-L^{2p})} (**2**) {[VO(OR)]₂(μ -*p*-L^{2m})} (R = *i*Pr **3**, *t*Bu **4**) have been prepared from [VO(OR)₃] (R = *n*Pr, *i*Pr or *t*Bu) and the respective phenol, namely 2,2'-ethylidenebis(4,6-di-*tert*-butylphenol) (L¹H₂) or $\alpha,\alpha,\alpha',\alpha'$ -tetra(3,5-di-*tert*-butyl-2-hydroxyphenyl)-*p/m*-xylene-*para*-tetraphenol (L^{2p/m}H₄). For comparative studies, the known complexes [VO(μ -O*n*Pr)L¹]₂ (**I**), [VOL³]₂ (**II**) (L³H₃ = 2,6-bis(3,5-di-*tert*-butyl-2-hydroxybenzyl)-4-*tert*-butylphenol) were prepared. An imido complex {[VCl(N*p*-tolyl)(NCMe)]₂(μ -*p*-L^{2p})} (**5**) has been prepared following work-up from [V(N*p*-tolyl)Cl₃] (L^{2p}H₄ and Et₃N). The molecular structures of complexes **1**–**5** are reported. Complexes **1**–**5** and **I** and **II** have been screened for their ability to ring open polymerise ϵ -caprolactone, L-lactide or rac-lactide with and without solvent present. The co-polymerization of ϵ -caprolactone with L-lactide or rac-lactide afforded co-polymers with low lactide content; the reverse addition was ineffective.

Received 23rd November 2015
Accepted 17th December 2015

DOI: 10.1039/c5ra24816g

www.rsc.org/advances

Introduction

As a biodegradable polyester that has the potential for replacing traditional polymers, polylactide (PLA) has attracted much attention in recent years.¹ ϵ -Caprolactone too is attracting interest as a precursor to biodegradable polycaprolactone (PCL) polymers.² Both types of polymer are readily formed *via* ring opening polymerization (ROP) of the respective monomer catalyzed by metal complexes, which can be a living process thereby allowing for good control. Given the bio-applications of PLA and PCL type polymers, there is a drive to develop syntheses using new catalysts that offer advantages over the established stannous octoate,³ yet which possess low toxicity. Furthermore, the properties associated with PLA and PCL can be quite different, as typified by their differences in elasticity, and so there is a drive to produce ϵ -CL/LA co-polymers of varying composition (and properties).

One metal attracting attention in polymerisation catalysis is vanadium.⁴ Given the toxicity associated with this metal is

relatively low,⁵ we have embarked upon a program to screen various vanadium systems for their ability to deliver, *via* ROP, biodegradable polymers with desirable properties. We note that reports on the use of group 5 complexes for the ROP of cyclic esters are scant.⁶ Herein, we investigate the potential of vanadyl complexes with ligands derived from di-(L¹H₂) or tetra-phenols (L^{2p/m}H₄) and for comparative studies the tri-phenol (L³H₃) (see Scheme 1) for the ROP of both L-lactide and ϵ -caprolactone and the co-polymerisation thereof, and report the effects of the structures of the complexes on the properties of the final polymeric products. Such chelating phenoxide ligation has proved useful in olefin polymerisation,⁴ but their use in the ROP of lactides and lactones, particularly that of the tri- and tetra-phenolic ligand sets, is rather limited.^{6d,7,8} Use of a tetra-phenolate ligand set, both *meta* and *para* forms, also allowed us to probe for possible cooperative effects, *viz.* **1** *versus* **2**–**4**. With this in mind, the crystal structures of the monomeric vanadyl complex [VO(O*t*Bu)L¹] (**1**) and the dinuclear vanadyl complexes {[VO(O*i*Pr)]₂(μ -*p*-L^{2p})} (**2**), {[VO(OR)]₂(μ -*p*-L^{2m})} (R = *i*Pr **3**, *t*Bu **4**) are also presented; the molecular structures of **I** and **II** have been reported elsewhere.⁹

Results and discussion

Vanadyl phenolate complexes

Interaction of [VO(O*t*Bu)₃] with the ethylidene-bridged di-phenol 2,2'-ethylidenebis(4,6-di-*tert*-butylphenol), 2,2'-CH₃CH[4,6-(*t*Bu)₂C₆H₂OH]₂ (LH₂) in refluxing toluene afforded, after workup, the monomeric complex [VO(O*t*Bu)L] (**1**) in good isolated yield (*ca.* 76%). Complex **1** is presumed to form *via*

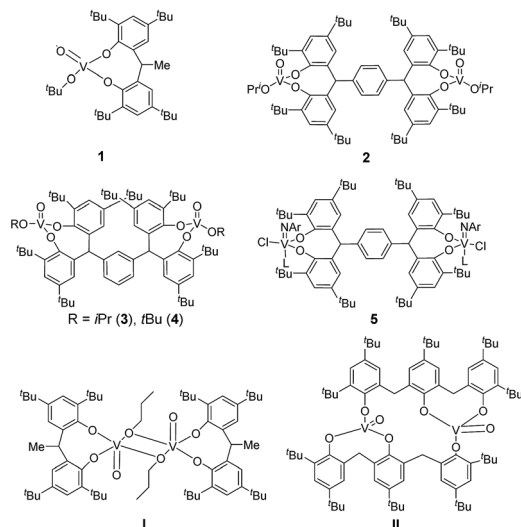
^aState Key Laboratory of Polymer Materials Engineering of China (Sichuan University), Polymer Research Institute of Sichuan University, Chengdu 610065, Sichuan, China. E-mail: jianglong@scu.edu.cn; Fax: +86-28-85402465; Tel: +86-28-85407286

^bDepartment of Chemistry, University of Hull, Hull, HU6 7RX, UK. E-mail: C.Redshaw@Hull.ac.uk; Fax: +44 (0)1482 466410; Tel: +44 (0)1482 465219

^cChemistry Department, Loughborough University, Leicestershire, LE11 3TU, UK

† Electronic supplementary information (ESI) available: ORTEPs and X-ray crystallographic files CIF format for the structure determinations of compounds **1**, **2**, 3·2CH₂Cl₂, 4·2CH₂Cl₂, 4·3CH₂Cl₂ and 5·2CH₃CN. CCDC 1040815, 1404533, 1404524–1404526 and 1404529. For ESI and crystallographic data in CIF or other electronic format see DOI: 10.1039/c5ra24816g





Scheme 1 Vanadyl complexes screened herein (Ar = *p*-tolyl, L = MeCN).

displacement of two molecules of *tert*-butanol in a similar fashion reported for related *n*-propoxide complexes.⁹ In the IR of **1**, there is a strong stretch at 1003 cm^{-1} assigned to the $\nu(\text{V}=\text{O})$ group. Crystals of **1** suitable for X-ray diffraction were readily grown from a saturated acetonitrile solution at $0\text{ }^{\circ}\text{C}$. The structure of **1** is shown in Fig. 1 (for ORTEP, see Fig. S1†), with selected bond lengths and angles given in the caption; crystal structure data are given in Table S2.† The vanadium centre adopts a distorted tetrahedral environment with angles varying from ideal in the range $107.7(2)$ to $112.1(2)^{\circ}$. The chelating ligand forms an eight membered metallocycle adopting a flattened chair conformation, with a bite angle of $110.1(2)^{\circ}$, which is somewhat larger than that found in the monomeric vanadyl complex $\{\text{VOCl}[2,2'\text{-CH}_2(4\text{-Me},6\text{-}t\text{BuC}_6\text{H}_2\text{O})_2]\}$ [$106.9(2)^{\circ}$] and

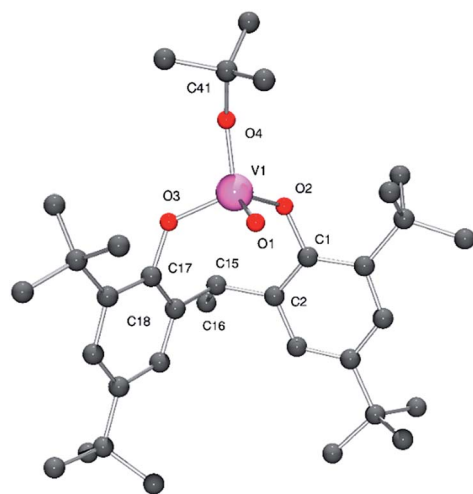


Fig. 1 Molecular structure of **1**. Selected bond lengths (Å) and angles ($^{\circ}$): V(1)–O(1) 1.789(5), V(1)–O(2) 1.783(5), V(1)–O(3) 1.581(5), V(1)–O(4) 1.739(5); O(1)–V(1)–O(2) $110.1(2)$, V(1)–O(1)–C(1) $124.4(4)$, V(1)–O(2)–C(17) $130.9(4)$, V(1)–O(4)–C(41) $145.9(5)$.

Table 1 Selected bond lengths for **3**, $4 \cdot 2\text{CH}_2\text{Cl}_2$ and $4 \cdot 3\text{CH}_2\text{Cl}_2$

Bond lengths (Å)/angles ($^{\circ}$)	3	$4 \cdot 2\text{CH}_2\text{Cl}_2$	$4 \cdot 3\text{CH}_2\text{Cl}_2$
V1–O(phenolate)	1.790(2)	1.7908(15)	1.790(6)
V1=O(vanadyl)	1.790(2)	1.7963(15)	1.806(5)
V1–O(alkoxide)	1.581(3)	1.5890(16)	1.577(6)
V2–O(phenolate)	1.733(3)	1.7298(16)	1.736(6)
V2–O(alkoxide)	1.791(2)	1.7891(16)	1.792(6)
V2=O(vanadyl)	1.793(2)	1.7904(15)	1.796(5)
V2–O(alkoxide)	1.584(3)	1.5908(17)	1.572(7)
O1–V1–O2		111.31(7)	
O2–V1–O5		106.92(8)	
O5–V1–O6		112.95(8)	
V1–O1–C1		126.91(13)	
V1–O16–C1		126.91(13)	
V1–O6–C65		143.63(15)	

Table 2 ^{51}V NMR spectroscopic data for compounds **1**–**5** and **I** and **II** (recorded in CDCl_3 at 298 K versus VOCl_3 as standard)

Compound	δ (ppm)	$\omega_{1/2}$ (Hz)
1	–482.4	63
I	–410.3 (ref. 4a)	—
II	–498	340 (ref. 4d)
2	–449.6	184
3	–449.6	190
4	–468.9	652
5	–218.9	1074

the dimeric complex $[\text{VO}(\text{OnPr})\text{L}]_2$ [$94.49(10)^{\circ}$].^{9a,10} The V–O bond lengths to the bisphenolate ligand [$1.789(5)$ and $1.783(5)$ Å] are typical of those previously observed for vanadium aryloxides,^{9,10} whilst the V–O alkoxide distance [$1.739(5)$ Å] is shorter than those typically observed in alkoxy vanadium complexes, but similar to that reported in the monomeric imido vanadium complex $[\text{V}(\text{NAr})(\text{OtBu})\text{L}]$ [$1.738(2)$ Å] (Ar = *p*-ClC₆H₄).¹¹ The alkoxide ligand is best described as bent with a V(1)–O(4)–C(40) angle of $145.9(5)^{\circ}$, which is slightly smaller than the analogous angle in the imido complexes $[\text{V}(\text{NAr})(\text{OtBu})\text{L}]$ [$146.77(12)$ – $151.9(2)^{\circ}$] (Ar = *p*-ClC₆H₄, *p*-tolyl).¹¹

Extension of this synthetic methodology to the tetra-phenol $\alpha,\alpha,\alpha',\alpha'$ -tetra(3,5-di-*tert*-butyl-2-hydroxyphenyl-*p*-xylene-*para*-tetra-phenol ($\text{L}^{2\text{P}}\text{H}_4$) afforded the dinuclear complex $\{[\text{VO}(\text{OiPr})_2(\mu\text{-}p\text{-L}^{2\text{P}})]\}$ (**2**) in good yield.

Crystals of **2** suitable for X-ray diffraction were readily grown from a saturated dichloromethane solution at $0\text{ }^{\circ}\text{C}$. The structure of **2** is shown in Fig. 2 (for ORTEP, see Fig. S2†), with selected bond lengths and angles given in the caption; crystal structure data are given in Table 5. The tetra-phenolate ligand is centrosymmetric with one vanadyl cation bound above the plane of the central aromatic ring and one beneath. The separation of these two identical metal centres is 11.756 Å . Each vanadium centre can be described as adopting a pseudo tetrahedral geometry. The bite angle formed by the tetra-phenolate at each vanadium is $109.4(2)^{\circ}$, which is slightly smaller than that observed for **1** ($110.1(2)^{\circ}$) and for the recently reported



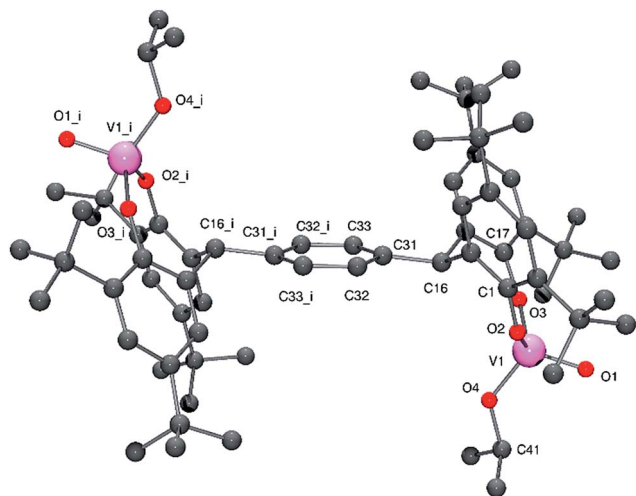


Fig. 2 Molecular structure of **2**. Selected bond lengths (Å) and angles (°): V1–O1 1.575(4), V1–O2 1.777(4), V1–O3 1.750(5), V1–O4 1.759(5); O2–V1–O3 109.4(2), V1–O2–C1 139.7(5), V1–O3–C17 151.7(4), V1–O4–C40 130.1(5).

alkoxide complexes $\{[\text{VO}(\text{OR})_2(\mu\text{-}p\text{-L}^{2\text{P}})]\}$ [$\text{R} = n\text{Pr}$, 111.73(7)°; $t\text{Bu}$, 112.0(2)°]; and the metallocycle adopts a flattened boat conformation. The isopropoxide ligand can be described as bent with a V2–O8–C68 angle of 130.1(5)°.

Similar use of the *meta* tetra-phenol $\alpha,\alpha,\alpha',\alpha'$ -tetra(3,5-di-*tert*-butyl-2-hydroxyphenyl-*m*-xylene-*meta*-tetra-phenol ($\text{L}^{2\text{m}}\text{H}_4$) with $[\text{VO}(\text{OR})_3]$ ($\text{R} = n\text{Pr}$ or $t\text{Bu}$) afforded the dinuclear complexes $\{[\text{VO}(\text{OR})_2(\mu\text{-}m\text{-L}^{2\text{m}})]\}$ ($\text{R} = i\text{Pr}$ **3**, $t\text{Bu}$ **4**) in good yield. Crystals of **3** and of **4** suitable for an X-ray diffraction studies were obtained on cooling (to -20°C) their respective saturated dichloromethane solutions. The molecular structure of **3**·2CH₂Cl₂ is shown in Fig. 3 (for ORTEP, see Fig. S3†), with selected bond lengths (Å) and angles (°) given in Table 1 where they are compared with those of **4**·2CH₂Cl₂ and **4**·3CH₂Cl₂.

In **3**, the vanadium centres can be described as adopting a pseudo tetrahedral geometry. The bite angle formed by the tetra-phenolate at each vanadium is 110.55(11)°, which is slightly larger than that observed for **1**; again the metallocycle adopts a chair-boat conformation. The iso-propoxide ligand can be described as bent with a V2–O8–C68 angle of 140.5(3)°; the V–O iso-propoxide bond lengths are similar to those observed elsewhere.¹²

For **4**·2CH₂Cl₂, there is one molecule of the complex and two molecules of CH₂Cl₂ (modelled by the Platon SQUEEZE

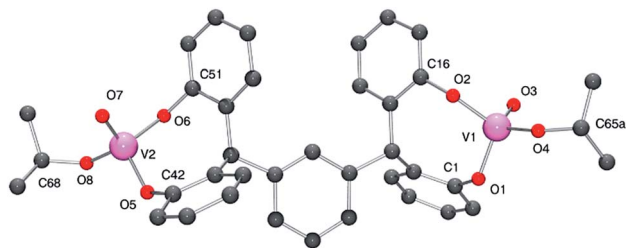


Fig. 3 Molecular structure of complex **3**·2CH₂Cl₂, indicating the atom numbering scheme. Hydrogen atoms and solvent molecules of crystallisation have been removed for clarity.

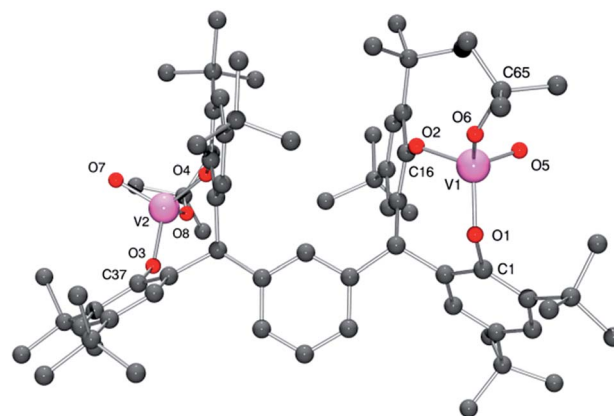


Fig. 4 Molecular structure of complex **4**·2CH₂Cl₂, indicating the atom numbering scheme. Hydrogen atoms and solvent molecules of crystallisation have been removed for clarity.

procedure) in the asymmetric unit.¹³ Each vanadium center adopts a pseudo-tetrahedral geometry (see Fig. 4; for ORTEP, see Fig. S4†), with bond angles in the range 106.92(8)–112.95(8)°; the bite angle of the chelate is 111.31(7)°. The *tert*-butoxide ligand is somewhat bent [V1–O6–C65 = 143.63(15)°], with a slightly larger angle than that observed in the isopropoxide **3** and presumably reflects the greater steric bulk of the *tert*-butoxide. The molecules pack in layers, however there is no significant interaction between the layers.

From a repeated synthesis of **4**, a different solvate was obtained, namely **4**·3CH₂Cl₂. In the molecular structure of **4**·3CH₂Cl₂, determined using synchrotron radiation,¹⁴ there is one well-defined dichloromethane which is involved in intramolecular interactions (see Fig. 5, for ORTEP, see Fig. S5†). In particular, there is a C–H···O H-bond to the oxo group O7 (see Table S1 in ESI† for geometry) and a C–H··· π interaction with the aromatic ring C51 > C56 {H(73B)···ring centroid = 2.56(2) Å}.

The known vanadyl complexes $[\text{VO}(\mu\text{-}On\text{Pr})\text{L}]_2$ (**I**), $[\text{VOL}^3]_2$ (**II**) were prepared as described previously ($\text{L}^3\text{H}_3 = 2,6\text{-bis}(3,5\text{-di-}tert\text{-butyl-2-hydroxybenzyl)-4-tert-butylphenol}$) *via* the reaction of $[\text{VO}(\text{OnPr})_3]$ and the respective chelating phenol.⁹

Vanadium imido phenolate complex

Given the oxo group is isoelectronic with the imido group, we extended the studies to the reaction of $[\text{V}(\text{Np-MeC}_6\text{H}_4)\text{Cl}_3]$,¹⁵ with $p\text{-L}^{2\text{P}}\text{H}_4$ in the presence of Et₃N. Following work-up (extraction into MeCN), the red/brown imido complex $\{[\text{V}(\text{Np-MeC}_6\text{H}_4)(\text{NCMe})\text{Cl}]_2(\mu\text{-}p\text{-L}^{2\text{P}})\} \cdot 2\text{MeCN}$ (**5**·2MeCN) was isolated in good yield. Single crystals of **5**, obtained on prolonged standing at ambient temperature, were subjected to an X-ray diffraction study. The structure of **5** is shown in Fig. 6 (for ORTEP, see Fig. S6†), with selected bond lengths and angles given in the caption. The geometry at each vanadium is best described as trigonal bipyramidal with the imido and MeCN groups occupying axial positions [N1–V1–N2 178.74(14)°]. Bond angles are in the range 111.59(11)–122.47(9)°, with the largest equatorial deviation associated with the angle subtended at the metal by the phenolic oxygen centres. The imido ligand has the



geometrical parameters associated with a linear imido function [V1–N1 1.670(3) Å; V1–N1–C40 170.5(3)°]. The structure of **5** closely resembles that of the recently reported complexes $\{[V(NAr)(THF)Cl]_2(\mu-p-L^{2p})\}$ (Ar = *p*-MeC₆H₄, *p*-CF₃C₆H₄), in which THF occupies one of the axial position at the metal as opposed to MeCN in **5**.^{4d}

⁵¹V NMR data for **1–5** and **I** and **II** are presented in Table 2, and all vanadyl complexes appear in the range δ –410 to –498 ppm, with the 5-coordinate VO₄ centre in **II** slightly upfield of the other 4-coordinate VO₃ containing species. The imido complex **5** appears somewhat downfield, a position which also reflects the presence of the chloride ligand; line widths are also increased in the presence of imido groups.¹⁵

Ring opening polymerisation (ROP) studies

ϵ -Caprolactone (ϵ -CL). Given its ease of preparation on a multi-gramme scale, complex **4** was used to determine the optimum conditions (temperature, time and concentration) needed for the ROP of ϵ -caprolactone. It was observed that the

ratio 200 : 1 for [CL] : [cat] was best both in the presence or absence of BnOH, over a period of 24 h at 80 °C. For all catalyst systems, runs conducted at temperatures of ≤ 45 °C or for ≤ 12 h led to either no polymer or low yields (see Table 3). All systems were relatively well behaved with only one run (run 3) affording a PDI of over 1.80, whilst the majority of runs were below 1.40. The presence of BnOH was also examined for **4** (runs 25–27), and under the optimized conditions, the conversion was about 10% lower whilst the observed M_n was about 30% lower. For **5**, bearing a terminal chloride ligand, the use of BnOH was beneficial in terms of % conversion, and the observed molecular weights (M_n) were also higher. In terms of pro-catalyst structure, there appeared to be no advantage in having two metals present given % conversion for **1** \approx **I** and **II** under optimized conditions (runs 3, 6 and 9). In the case of the tetraphenolate systems, it appears that use of systems (**3** and **4**) derived from the *meta* pro-ligand set *m*-L^{2m}H₄ are more effective than those (**2**) derived from the *para* pro-ligand *p*-L^{2p}H₄ (runs 13–15 and 16–26 *versus* 10–12) Table 3. This suggests in **3** and **4**

Table 3 Ring-opening polymerization of ϵ -caprolactone catalyzed by the vanadyl phenolate complexes **1–4**, the imido complex **5**, and the known complexes **II** and **III**

Run ^a	Cat	Temp/°C	Time/h	[CL] ₀ : [Cat] ₀ : [BnOH] ₀	Conv. ^b (%)	$M_{n,GPC}$ ^c	$M_{n,cal}$ ^d	PDI ^e
1	1	45	24	200 : 1 : 0	84	2440	19 400	1.11
2	1	60	24	200 : 1 : 0	99	4450	22 600	1.43
3	1	80	24	200 : 1 : 0	99	5430	22 600	2.01
4	I	45	24	200 : 1 : 0	98	4600	22 370	1.15
5	I	60	24	200 : 1 : 0	99	5760	22 600	1.80
6	I	80	24	200 : 1 : 0	98	5110	25 600	1.66
7	II	45	24	200 : 1 : 0	98	2860	22 370	1.20
8	II	60	24	200 : 1 : 0	98	3040	22 370	1.14
9	II	80	24	200 : 1 : 0	99	5950	22 600	1.32
10	2	45	24	200 : 1 : 0	55	1620	12 560	1.17
11	2	60	24	200 : 1 : 0	95	2850	21 830	1.20
12	2	80	24	200 : 1 : 0	99	4110	22 600	1.14
13	3	45	24	200 : 1 : 0	—	—	—	—
14	3	60	24	200 : 1 : 0	49	1610	11 410	1.15
15	3	80	24	200 : 1 : 0	99	2880	22 600	1.35
16	4	80	1	200 : 1 : 0	—	—	—	—
17	4	80	6	200 : 1 : 0	49	1120	11 410	1.12
18	4	80	12	200 : 1 : 0	89	2500	20 320	1.23
19	4	45	24	200 : 1 : 0	—	—	—	—
20	4	60	24	200 : 1 : 0	50	1620	11 560	1.12
21	4	80	24	100 : 1 : 0	89	2140	10 270	1.16
22	4	80	24	200 : 1 : 0	99	3520	22 740	1.33
23	4	80	24	400 : 1 : 0	99	4920	45 200	1.42
24	4	80	24	600 : 1 : 0	99	5720	67 800	1.47
25	4	45	24	200 : 2 : 1	10	800	2280	1.13
26	4	60	24	200 : 2 : 1	97	1200	22 250	1.29
27	4	80	24	200 : 2 : 1	99	2510	22 710	1.30
28	5	45	24	200 : 1 : 0	—	—	—	—
29	5	60	24	200 : 1 : 0	97	2170	22 370	1.16
30	5	80	24	200 : 1 : 0	99	3150	22 600	1.21
31	5	45	24	200 : 2 : 1	—	440	—	1.16
32	5	60	24	200 : 2 : 1	99	3260	22 710	1.14
33	5	80	24	200 : 2 : 1	99	5780	22 710	1.43

^a All reactions were carried out in toluene under nitrogen. ^b Determined by ¹H NMR. ^c M_n values were determined by GPC in THF vs. PS standards and were corrected with a Mark–Houwink factor of 0.56. ^d Calculated by (F.W. monomer \times [monomer]/[cat]) \times conversion + F.W. BnOH. ^e (M_w/M_n) were determined by GPC.



Table 4 Ring-opening polymerisation of ϵ -caprolactone catalysed by vanadyl phenolate complexes 1–4, imido complex 5 and known complexes I and II in the absence of solvent

Run	Cat	Time/min	[CL] ₀ : [Cat] ₀ : [BnOH] ₀	$M_{n,GPC}^a$	$M_{n,cal}^b$	PDI ^c	Conv. (%)
1	1	20	200 : 1 : 0	16 270	22 600	1.45	99
2	I	20	200 : 1 : 0	4930	22 600	1.26	99
3	II	30	200 : 1 : 0	11 740	21 690	1.62	95
4	2	30	200 : 1 : 0	7200	22 140	1.34	97
5	3	30	200 : 1 : 0	7130	21 910	1.50	96
6	4	40	200 : 1 : 0	2660	22 370	1.20	98
7	5	30	200 : 1 : 1	14 050	22 250	1.49	97
8	5	60	200 : 1 : 0	—	—	—	—

^a M_n values were determined by GPC in THF vs. PS standards and were corrected with a Mark-Houwink factor of 0.56. ^b (F.W. monomer \times [monomer]/[cat]) \times conversion + F.W. BnOH. ^c M_w/M_n were determined by GPC.

that there is a favourable V...V separation, which may favour the coordination of a single monomer to both catalytic centres of the same complex. One centre can then be used as a Lewis acid and the other using its V-OR functionality to attack the carbonyl

group. The chloride complex 5, in the presence of BnOH, afforded the highest yield (85%).

In the ¹H NMR spectra of the resulting PCL (e.g. see ESI, Fig. S7[†]), for runs involving pro-catalysts with a V-OR moiety

Table 5 Ring-opening polymerisation of L-lactide catalysed by vanadyl phenolate complexes 1–4, imido complex 5 and known complexes I and II

Run ^a	Cat	Temp/°C	Time/h	[LA] ₀ : [Cat] ₀ : [BnOH] ₀	Conv. ^b (%)	$M_{n,GPC}^c$	$M_{n,cal}^d$	PDI ^e
1	1	45	31	200 : 1 : 0	—	—	—	—
2	1	60	24	200 : 1 : 0	10	1480	2880	1.57
3	1	80	6	200 : 1 : 0	—	—	—	—
4	1	80	24	200 : 1 : 0	54	2310	15 570	1.24
5	1	80	35	200 : 1 : 0	50	2100	14 410	1.26
6	I	45	34	200 : 1 : 0	—	—	—	—
7	I	60	34	200 : 1 : 0	—	—	—	—
8	I	80	6	200 : 1 : 0	—	—	—	—
9	I	80	24	200 : 1 : 0	54	2930	15 850	1.73
10	I	80	31	200 : 1 : 0	54	2640	15 850	1.16
11	II	60	34	200 : 1 : 0	—	—	—	—
12	II	80	6	200 : 1 : 0	—	—	—	—
13	II	80	24	200 : 1 : 0	58	3010	16 720	1.46
14	II	80	34	200 : 1 : 0	60	3440	17 300	1.31
15	2	60	31	200 : 1 : 0	—	—	—	—
16	2	80	6	200 : 1 : 0	—	—	—	—
17	2	80	24	200 : 1 : 0	50	2120	14 410	1.34
18	2	80	36	200 : 1 : 0	58	2190	16 720	1.30
19	3	45	33	200 : 1 : 0	—	—	—	—
20	3	60	35	200 : 1 : 0	—	—	—	—
21	3	80	6	200 : 1 : 0	—	—	—	—
22	3	80	24	200 : 1 : 0	15	1340	4320	1.11
23	3	80	36	100 : 1 : 0	52	2150	7490	1.11
24	3	80	36	200 : 1 : 0	52	2510	14 990	1.09
25	3	80	36	400 : 1 : 0	60	34 590	34 590	1.26
26	3	80	36	600 : 1 : 0	62	3760	53 620	1.29
27	3	110	31	200 : 1 : 0	51	2010	14 700	1.26
28	4	60	30	200 : 1 : 0	9	870	2590	1.23
29	4	80	6	200 : 1 : 0	—	—	—	—
30	4	80	24	200 : 1 : 0	20	1930	5760	1.01
31	4	80	31	200 : 1 : 0	45	2460	12 970	1.10
32	5	80	31	200 : 1 : 0	—	—	—	—
33	5	80	6	200 : 1 : 1	—	—	—	—
34	5	80	24	200 : 1 : 1	53	3400	15 380	1.29
35	5	110	31	200 : 1 : 1	55	3640	15 960	1.35

^a All reactions were carried out in toluene under nitrogen. ^b Determined by ¹H NMR. ^c M_n values were determined by GPC in THF vs. PS standards and were corrected with a Mark-Houwink factor of 0.58. ^d (F.W. monomer \times [monomer]/[cat]) \times conversion + F.W. BnOH. ^e (M_w/M_n) were determined by GPC.



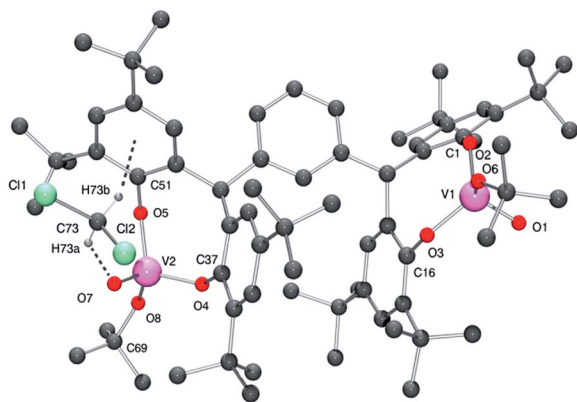


Fig. 5 Molecular structure of complex **4** · 3CH₂Cl₂, indicating the atom numbering scheme. Hydrogen atoms except those on the CH₂Cl₂ have been removed for clarity.

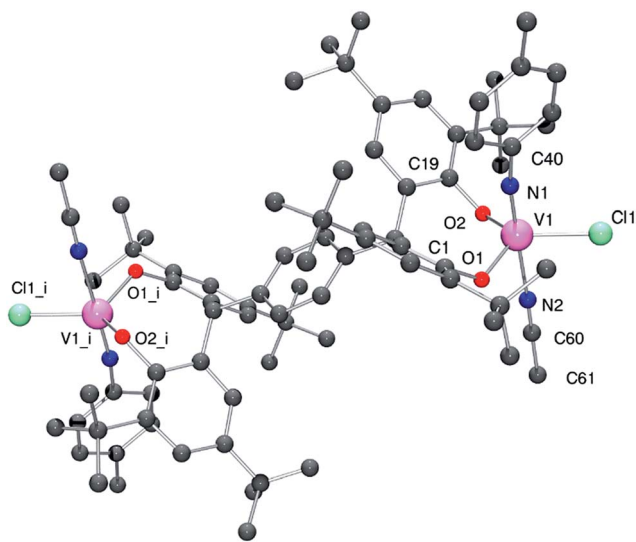


Fig. 6 Molecular structure of complex **5** · 2MeCN, indicating the atom numbering scheme. Hydrogen atoms and solvent molecules of crystallisation have been removed for clarity. Selected bond lengths (Å) and angles (°): V1–N1 1.670(3), V1–O1 1.818(3), V1–O2 1.831(2), V1–C1 2.2609(11); O1–V1–N1 98.33(13), O1–V1–O2 111.59(11), Cl1–V1–N1 94.74(11), V1–O1–C1 124.4(2), V1–O2–C19 121.4(2), V1–N1–C50 170.5(3). Symmetry operation used to generate equivalent atoms: *i* = –*x*, –*y*, –*z*.

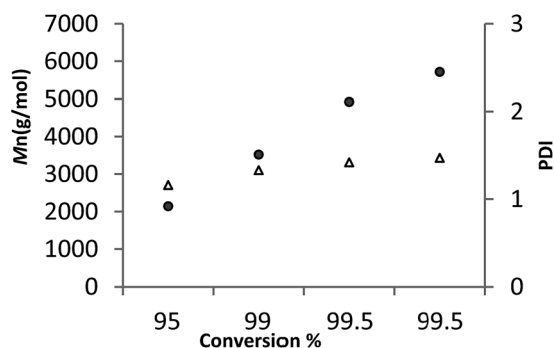


Fig. 7 M_n (●) and M_w/M_n (Δ) vs. monomer conversion in the ROP of ϵ -CL.

present, signals were assignable to a hydroxyl end group (CH₂OH) and an alkyl ester (*e.g.*, isopropyl ester for **3**). This indicated that the polymerization procedure involved rupture of the monomer acyl–oxygen bond and insertion in the alkoxide–vanadium bond. For runs conducted in the presence of BnOH, ¹H NMR spectra were more complicated in terms of end group, with both OBn and OR (*e.g.* *t*-Bu for **4**) present (see ESI, Fig. S8†).

Interestingly, in the absence of solvent, these systems performed far better at 80 °C, with conversions \geq 95%, polydispersities \leq 1.62 (see Table 4) and in general afforded higher observed molecular weight (M_n) polymers (see Table 4). The monomeric *tert*-butoxide complex **1** was found to afford the best yield (90%) and highest molecular weight (M_n) PCL (\sim 16 300). By contrast, **III** afforded lowest conversion and highest PDI, which we assume is due to the lack of a readily accessible alkoxide bond (a phenoxide linkage of the tri-phenolate would need to be broken). Interestingly, the isopropoxides **2** and **3** gave very similar results, whilst the *tert*-butoxide **4** afforded a polymer of much lower molecular weight (M_n). For complex **5**, it was necessary to add an equivalent of BnOH to achieve ROP activity (run 7 vs. 8, Table 4), and the resulting polymer was of higher molecular weight (M_n) \sim 14 000 g mol^{–1}.

In general for the CL runs, despite the narrow polydispersity, the polymer molecular weights (M_n) were much lower than expected, indicating in all cases that significant *trans*-esterification reactions were occurring. Further evidence was provided by the MALDI-ToF mass spectra where, as well as the major population of peaks, there was evidence of a second, albeit minor, population (see ESI, Fig S9–S12† in toluene; Fig. S13 and S14,† no solvent).

For **6**, a plot of average molecular weight (M_n) versus against conversion (Fig. 7, runs 21–24 Table 3) exhibited a linear relationship. Given the plot also shows that the PDI remained narrow, it suggests that under these conditions the ROP by **6** is proceeding in a living manner.

The production of only low molecular weight polymers using alkoxy vanadium systems has been noted previously.⁹ Herein, there was little correlation of ⁵¹V NMR signal (Table 2) versus catalytic activity (see ESI, Fig. S15†).

L-Lactide (L-LA). Complexes **1** to **5** and **II** and **III** have been screened for their potential to act as catalysts for the ROP of L-lactide. In this case, complex **3** was chosen to establish the optimized conditions for the ROP of L-lactide (L-LA). Using a ratio of 200 : 1 for L-LA to pro-catalyst, it was found that at temperatures below 80 °C, there was no catalytic activity even after 35 h. At 80 °C, there was no activity after 6 h, and polymer was only isolated at 24 h affording a yield of 20%. Prolonging the reaction time increased the yield to 50%. Further increasing the temperature to 110 °C afforded only a slight improvement in yield, with a slight increase in PDI. Varying the ratio of L-LA to pro-catalyst led to a slight improvement in the yield (55%), together with an increase in the molecular weight (M_n) and a slight broadening of the PDI. Given these results, the other complexes were screened using a ratio of 200 : 1 for L-LA to pro-catalyst, and in the case of **5**, screening was conducted both in the absence and presence of BnOH (see Table 5).



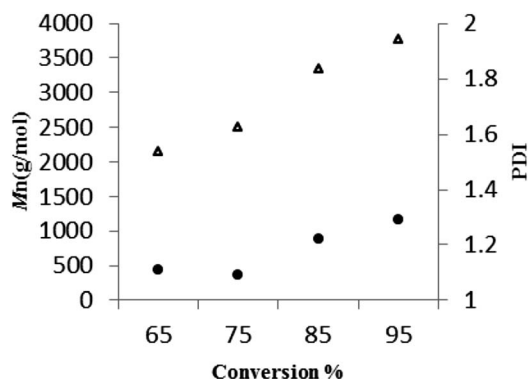


Fig. 8 M_n (Δ) and M_w/M_n (●) vs. monomer conversion in the ROP of L-LA.

In the case of **4**, differing from **3** only in the nature of the alkoxide (*tert*-butoxide *versus* isopropoxide) there was some activity at 60 °C over 30 h, though the yield was low (10%). Reactions conducted at 80 °C afforded yields slightly lower than observed for **3**; molecular weights (M_n) were similar. In the case of complex **2**, which differs from **3** in the nature of the tetraphenolate employed (*i.e.* *para* *versus* *meta*), activity was observed at 80 °C on prolonging the reaction time. Yields using **2** after 24 h were typically higher than for **3**, but then after 36 h, the yields were approximately the same (slightly higher using **3**); molecular weights (M_n) followed the same trend. PDIs for runs employing **2** were higher than those for **3**. However, these results, unlike those for ϵ -caprolactone, did not suggest that use of the *meta* ligand had any beneficial effect in terms of the

distance between the two vanadium centres and the resultant ROP activity. In the case of the imido complex **5** (a chloride complex), it proved necessary here to add BnOH to afford an active system. We note however that chlorides have previously been shown to be capable of the ROP of lactide.¹⁶ At 80 °C, activity was observed after 24 h, with yields similar to the vanadyl complex **2**, but with higher molecular weight (M_n) polymers formed.

Comparing results for **1** *versus* **I** suggests that there is no benefit in having two vanadyl centers present rather than one. Indeed, results for **1** suggest the opposite given that **1** can operate at 60 °C and also affords superior yields at 80 °C. Results for **III** are similar to those of **II**.

In all cases, observed molecular weights (M_n) are far lower than calculated values. In contrast to the ϵ -caprolactone screening, conducting the L-LA ROP runs in the absence of any solvent did not afford improved results and actually afforded little or no polymer.

As for PCL, the observed molecular weights (M_n) for the PLA are lower than the calculated values, and in the MALDI-ToF spectra (see ESI, Fig. S16–S18†) there was evidence of a second population consistent with some transesterification processes occurring.

For **3**, a plot (Fig. 8, runs 23–26, Table 5) of the average molecular weight (M_n) of the poly(L-LA) as a function of the monomer conversion was linear, and with consistently low PDI values suggestive of a living process.

rac-Lactide (rac-LA). Complexes **1–5** and **I** and **II** were also screened for their ability to ROP *rac*-lactide and the results are given in Table 6. Temperatures of at least 80 °C were found necessary to achieve activity and yields were found to be at best

Table 6 Ring-opening polymerization of *rac*-lactide catalyzed by vanadyl phenolate complexes **1–4**, imido complex **5**, and known complexes **I** and **II**

Run ^a	Cat	Temp/°C	Time/h	[LA] ₀ : [Cat] ₀ : [BnOH] ₀	Conv. ^b (%)	$M_{n,GPC}$ ^c	$M_{n,cal}$ ^d	PDI ^e	Pr ^f
1	1	80	24	200 : 1 : 0	80	6050	23 060	1.30	0.61
2	I	60	24	200 : 1 : 0	—	—	—	—	—
3	I	80	24	200 : 1 : 0	70	3650	20 180	1.15	0.60
4	II	60	24	200 : 1 : 0	—	—	—	—	—
5	II	80	24	200 : 1 : 0	78	3860	22 480	1.09	0.63
6	2	60	24	200 : 1 : 0	—	—	—	—	—
7	2	80	24	100 : 1 : 0	65	1460	9370	1.13	—
8	2	80	24	200 : 1 : 0	80	2720	23 060	1.19	0.58
9	2	80	24	400 : 1 : 0	75	3450	43 240	1.24	0.58
10	2	80	24	600 : 1 : 0	75	3570	64 860	1.23	0.58
11	2	110	24	200 : 1 : 0	75	2440	21 620	1.21	0.58
12	3	60	24	200 : 1 : 0	—	—	—	—	—
13	3	80	12	200 : 1 : 0	44	790	12 970	1.17	—
14	3	80	24	200 : 1 : 0	83	2860	25 940	1.18	0.58
15	3	110	24	200 : 1 : 0	75	2480	21 620	1.27	0.61
16	4	80	24	200 : 1 : 0	79	2120	23 060	1.25	0.61
17	4	110	24	200 : 1 : 0	75	4120	21 620	1.23	0.61
18	5	80	24	200 : 1 : 1	—	—	—	—	—
19	5	110	24	200 : 1 : 1	78	2210	22 590	1.10	0.58
20	5	130	24	200 : 1 : 0	—	—	—	—	—

^a All reactions were carried out in toluene under nitrogen. ^b Determined by ¹H NMR. ^c M_n values were determined by GPC in THF vs. PS standards and were corrected with a Mark–Houwink factor of 0.58. ^d Calculated from (F.W. monomer × [monomer]/[cat]) × conversion + F.W. BnOH. ^e M_w/M_n were determined by GPC. ^f Determined by analysis of the tetrad signal in the ¹H NMR spectrum.



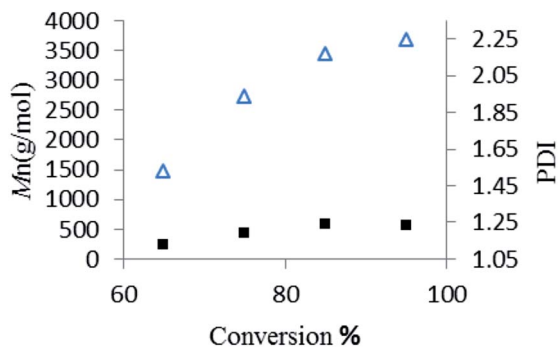


Fig. 9 M_n (Δ) and M_w/M_n (\bullet) vs. monomer conversion in the ROP of *rac*-LA.

moderate $\leq 50\%$ as found for *l*-lactide. The ROP appeared to be well controlled in terms of PDI with values in the range 1.09–1.30 observed (Fig. 9). There was no obvious advantage in the use of *meta* vs. *para* ligation in **2** and **3** at either 80 or 110 °C. Looking at **3** vs. **4** (OiPr vs. OiBu), at 80 °C, the isopropoxide **3** afforded higher molecular polymer (M_n) in higher yield, whereas at 110 °C the trend was reversed.

Observed molecular weights (M_n) were again lower than calculated values, and MALDI-ToF spectra (e.g. Fig. S19, ESI†) also revealed a number of minor populations.

As for *l*-lactide, use of no solvent afforded little or no observed catalytic activity.

To assign the stereochemistry of the PLA polymers we employed 2D *J*-resolved ^1H NMR spectroscopy and assigned the peaks by reference to the literature.¹⁷ Representative spectra for runs **1**, **5** and **17** are given in the ESI (Fig. S20–S22†), with the assignments given on the respective figures. These systems gave moderately isotactic PLA with a Pr value in the range 0.58–0.63.

Runs conducted in different solvents, namely THF and CH_2Cl_2 resulted in little or no polymer.

The presence of cyclic PLA was ruled out by comparison with literature MALDI-ToF and ^1H NMR spectra.¹⁸

Co-polymerisation of ϵ -caprolactone and *l*-lactide. Complexes **1** to **5** and **I** and **II** have also been screened for their potential to act as catalysts for the co-polymerisation of CL with

Table 8 Synthesis of diblock copolymers from cyclic ester monomers (LA = *rac*-lactide)

Run ^a	Complex	CL : LA ^b	Yield%	M_n^c	M_w/M_n^d
1	1	382 : 18	88	5850	1.42
2	I	375 : 25	73	3210	1.92
3	II	363 : 73	70	3910	1.21
4	2	360 : 40	75	3260	1.71
5	3	375 : 25	68	3840	1.60
6	4	367 : 33	60	3270	1.46
7	5	343 : 57	70	1770	1.18

^a All reactions were carried out in toluene under nitrogen under optimum condition 24 h CL/24 h *rac*-LA (80 °C). ^b Ratio of LA to CL observed in the co-polymer by ^1H NMR spectroscopy. ^c M_n values were determined by GPC in THF vs. PS standards and were corrected with a Mark–Houwink factor ($M_{n,\text{GPC}} \times 0.56 \times \% \text{PCL} + M_{n,\text{GPC}} \times 0.58 \times \% \text{PLLA}$). ^d PDI were determined by GPC.

l-lactide under the optimized conditions found for the homo-polymerisations in toluene, i.e. 80 °C, 200 : 200 : 1 for CL : LA : pro-cat over 24 h ($\times 2$). In all cases (Table 7), good yields (65–83%) of co-polymer were formed, but with low lactide content (2.5–9.0%) as observed from ^1H NMR spectra (ESI, Fig. S23†); the highest % incorporation of LA (9%) was found for **7** in the presence of BnOH. In the ^1H NMR, the end groups for alkoxide and hydroxyl were also evident. Observed molecular weights were in general higher than those observed for the homo-polymerisations conducted in toluene. Thermal analysis of the co-polymer by DSC revealed two melting points at 55.1 °C (PCL) and 170.5 °C (PLA), see ESI Fig. S24.† If the addition of the monomers was reversed, i.e. *l*-LA added first, no co-polymer was isolated after work-up. This suggested that a PLA chain end was not capable of PCL chain growth.

Co-polymerisation of ϵ -caprolactone and *rac*-lactide. Co-polymerisations involving CL and *rac*-LA gave similar results to the co-polymerisation with *l*-LA – see Table 8. Yields were in the range 60–88% and the incorporation of *rac*-lactide was 4.5–14.3%, and again the highest incorporation was noted for **5**. In the ^1H NMR spectrum, the end groups for alkoxide and hydroxyl were also evident, see ESI Fig. S25.† We also recorded the DSC (see Fig. S26, ESI†) which, as for the co-polymerization of CL and *l*-LA revealed two peaks: a large peak at 55.09 and a much smaller peak at 170.49.

Given the low molecular weight products isolated during these studies, the presence of impurities (e.g. lactic acid from non-recrystallized *rac*-lactide) acting as chain transfer agents (or co-initiator) cannot be ruled out. However, we note that there is interest in low molecular weight poly(lactide/caprolactone) polymers as bio adhesives.¹⁹

Conclusions

In conclusion, we have examined the ROP behaviour of a series of vanadyl complexes bearing chelating di-, tri- and tetra-phenolate ligands towards ϵ -caprolactone, *l*-lactide or *rac*-lactide with and without solvent present, and the co-polymerisation of ϵ -CL with lactide. For the homo-polymerisation of ϵ -CL, under

Table 7 Synthesis of diblock copolymers from cyclic ester monomers (LA = *l*-lactide)

Run ^a	Complex	CL : LA ^b	Yield%	M_n^c	M_w/M_n^d
1	1	390 : 10	83	15 740	1.87
2	I	383 : 17	77	3840	1.24
3	II	379 : 21	68	3600	1.16
4	2	385 : 15	73	4890	1.54
5	3	383 : 17	71	4560	1.66
6	4	380 : 20	66	5790	1.43
7	5	364 : 46	65	3400	1.26

^a All reactions were carried out in toluene under nitrogen under optimum condition 24 h CL/24 h *l*-LA (80 °C). ^b Ratio of LA to CL observed in the co-polymer by ^1H NMR. ^c M_n values were determined by GPC in THF vs. PS standards and were corrected with a Mark–Houwink factor ($M_{n,\text{GPC}} \times 0.56 \times \% \text{PCL} + M_{n,\text{GPC}} \times 0.58 \times \% \text{PLLA}$). ^d PDI were determined by GPC.



the optimized conditions in toluene, yields were typically of the order of 70%. It was observed that there was no advantage in having two metals present (*cf.* to one), whilst for the tetraphenolates use of the *meta* ligand set appeared beneficial (*cf.* the *para* ligand set), which perhaps reflects the closer proximity of the metal centres in the former. Conducting the runs in the absence of solvent led to higher conversions, typically >95%. For the ROP of L-lactide, the performances of 1–5 (and I and II) were not so good, affording PLA in only low to moderate ($\leq 55\%$) yields at higher temperatures and over prolonged reaction periods. There was no evidence of any beneficial cooperative effects and conducting the runs in the absence of solvent afforded no improvement. Results for *rac*-lactide were similar to L-lactide; 2D J-resolved ^1H NMR spectroscopy indicated the formation of moderately isotactic PLA. Co-polymerisation of CL with L-lactide afforded good yields (65–83%) of co-polymer, but with low lactide content (2.5–9.0%); reversing the order of monomer addition resulted in no product. Similar results were observed for co-polymerisation of CL with *rac*-lactide.

Experimental

General

All manipulations were carried out under an atmosphere of dry nitrogen using conventional Schlenk and cannula techniques or in a nitrogen-filled glove box. Diethyl ether and tetrahydrofuran were refluxed over sodium and benzophenone. Toluene was refluxed over sodium. Dichloromethane and acetonitrile were refluxed over calcium hydride. All solvents were distilled and degassed prior to use. IR spectra (nujol mulls, KBr or NaCl windows) were recorded on a Nicolet Avatar 360 FT IR spectrometer; ^1H NMR spectra were recorded at room temperature on a Varian VXR 400 S spectrometer at 400 MHz or a Gemini 300 NMR spectrometer or a Bruker Advance DPX-300 spectrometer at 300 MHz. The ^1H NMR spectra were calibrated against the residual protio impurity of the deuterated solvent. Elemental analyses were performed by the elemental analysis service at the London Metropolitan University or the University of Hull. Matrix Assisted Laser Desorption/Ionization-Time of Flight (MALDI-ToF) mass spectrometry was performed on Bruker autoflex III smart beam in linear mode. MALDI-ToF mass spectra were acquired by averaging at least 100 laser shots. 2,5-Dihydroxybenzoic acid was used as matrix and tetrahydrofuran as solvent. Sodium chloride was dissolved in methanol and used as the ionizing agent. Samples were prepared by mixing 20 μl of polymer solution in tetrahydrofuran (2 mg ml^{-1}) with 20 μl of matrix solution (10 mg ml^{-1}) and 1 μl of a solution of ionizing agent (1 mg ml^{-1}). Then 1 ml of these mixtures was deposited on a target plate and allowed to dry in air at room temperature. L-Lactide (99.7%, with D-lactide content less than 1%) was provided by Shenzhen Brightchina Industrial Co. Ltd (Shenzhen, China) as monomer. *rac*-Lactide and ϵ -caprolactone were purchased from Sigma Aldrich and were used as received. Benzyl alcohol was distilled over CaH_2 under vacuum. Other solvents were all of analytical grade and provided by Kelong Chemical Reagent Factory of Chengdu (Chengdu, China), and

were used without further purification unless noted. Complexes I and II were prepared as reported in the literature.¹¹

Synthesis of [VO(O*t*Bu)₃] (1). LH_2 (2.0 g, 4.58 mmol) and [VO(O*t*Bu)₃] (1.32 g, 4.61 mmol) were refluxed in toluene (30 ml) for 12 h. Upon cooling, volatiles were removed *in vacuo*, and the product extracted using warm acetonitrile (30 ml). Upon standing overnight for 12 h at 0 °C, red/brown prisms formed. Yield (1.96 g, 76%). IR (cm^{-1}): 3487w, 1567w, 1417m, 1361s, 1292s, 1240w, 1229w, 1214w, 1199w, 1190w, 1155m, 1125m, 1108s, 1013s, 1003s, 978m, 876w, 845w, 799s, 767w, 722m, 636w. Found: C, 70.69; H 9.35. $\text{C}_{34}\text{H}_{53}\text{VO}_4$ requires C, 70.81; H, 9.26%. ^1H NMR (CDCl_3 , 400 MHz): δ : 7.51–7.16 (overlapping m, 4H, arylH), 5.08 (q, 1H, J_{HH} 8.0 Hz, $\text{CH}_{\text{bridge}}$), 1.71 (s, 9H, O*t*Bu), 1.58 (d, 3H J_{HH} 8.0 Hz, $\text{CH}_3_{\text{bridge}}$), 1.42 (s, 18H, *t*Bu), 1.33 (s, 18H, *t*Bu). ^{51}V NMR (CDCl_3 , 298 K): -482.4 ($w_{1/2} = 63$ Hz).

Synthesis of $\{\text{L}^{3\text{P}}[\text{VO}(\text{iPrO})_2\} \cdot 2\text{CH}_2\text{Cl}_2 \cdot (2 \cdot 2\text{CH}_2\text{Cl}_2)$. $\text{L}^{2\text{P}}\text{H}_4$ (4.1 g, 4.44 mmol) and VO(*i*PrO)₃ (2.10 ml, 8.90 mmol) were refluxed in toluene (30 ml) for 12 h. On cooling, volatiles were removed *in vacuo* and the residue was extracted into dichloromethane (30 ml). Prolonged standing at 0 °C afforded 2 as a brown solid in 4.32 g, 83% yield. $\text{C}_{70}\text{H}_{100}\text{V}_2\text{O}_8 \cdot \frac{3}{4}\text{CH}_2\text{Cl}_2$ (sample dried *in vacuo* for 2 h) requires C 68.80, H, 8.28. Found C, 68.66, H 8.29%. MS (solid, ASAP technique): m/z 1171.5 $[\text{M}]^+$, 1111.6 $[\text{M} - \text{O}i\text{Pr}]^+$, 1069.5 $[\text{M} - \text{O}i\text{Pr} - i\text{Pr}]^+$. IR: 1572w, 1408w, 1260s, 1225w, 1189w, 1149w, 1093bs, 1019bs, 873w, 862w, 799s, 722w, 663w, 601w. ^1H NMR (CDCl_3): $\delta = 7.38$ – 7.14 (overlapping m, 8H, arylH), 6.77 (s, 4H, arylH), 6.33 (s, 2H, CH), 5.64 (sept, $^3J_{\text{HH}}$ 4.0 Hz, 2H, CHMe_2), 5.29 (s, 4H, CH_2Cl_2), 1.61 (d, $^3J_{\text{HH}}$ 4.0 Hz, 12H, CHMe_2), 1.44 (s, 36H, $\text{C}(\text{CH}_3)_3$), 1.23 (s, 36H, $\text{C}(\text{CH}_3)_3$). ^{51}V NMR (CDCl_3) $\delta = -449.7$ ($w_{1/2} = 688$ Hz).

Synthesis of $\{\text{L}^{3\text{m}}[\text{VO}(\text{O}i\text{Pr})_2\} \cdot 2\text{CH}_2\text{Cl}_2 \cdot (3 \cdot 2\text{CH}_2\text{Cl}_2)$. As for 2, but using $\text{L}^{2\text{m}}\text{H}_4$ (4.1 g, 4.4 mmol) and [VO(*i*PrO)₃] (2.10 ml, 8.90 mmol) affording 3 as a brown solid, yield 3.87 g, 66%. Crystals suitable for X-ray diffraction were obtained on cooling (-20 °C) of a saturated dichloromethane solution. $\text{C}_{70}\text{H}_{98}\text{V}_2\text{O}_8 \cdot \frac{1}{2}\text{CH}_2\text{Cl}_2$ (sample dried *in vacuo* for 12 h) requires C 68.93, H, 8.07. Found C, 68.66, H 8.29%. MS (solid, APCI): 1170.6 $[\text{MH}]^+$, 1111.5 $[\text{MH} - \text{O}i\text{Pr}]^+$, 1068.5 $[\text{MH} - \text{O}i\text{Pr} - i\text{Pr}]^{2+}$. IR: 1598m, 1568w, 1406m, 1376s, 1361s, 1325m, 1290m, 1263s, 1237m, 1222s, 1196m, 1104bs, 1005bs, 981bs, 928w, 911m, 860m, 844s, 810m, 797m, 780m, 769s, 740m, 722m, 698w, 669m, 648w, 607m. ^1H NMR (CDCl_3): $\delta = 7.25$ – 7.14 (overlapping m, 6H, arylH), 6.78 (m, 2H, arylH), 6.62 (s, 2H, arylH), 6.27 (s, 2H, CH), 5.62 (sept, $^3J_{\text{HH}}$ 4.0 Hz, 2H, CHMe_2), 5.29 (s, 4H, CH_2Cl_2), 1.61 (d, $^3J_{\text{HH}}$ 4.0 Hz, 12H, CHMe_2), 1.40 (s, 36H, $\text{C}(\text{CH}_3)_3$), 1.17 (s, 36H, $\text{C}(\text{CH}_3)_3$). ^{51}V NMR (CDCl_3): $\delta = -449.9$ ($w_{1/2} = 688$ Hz).

Synthesis of $\{[\text{VO}(\text{tBuO})_2](\mu\text{-}m\text{-L}^{3\text{m}})\} \cdot 2\text{CH}_2\text{Cl}_2 \cdot (4 \cdot 2\text{CH}_2\text{Cl}_2)$. As for 2, but using [VO(*t*BuO)₃] (3.20 g, 8.90 mmol) and $m\text{-L}^{3\text{m}}\text{H}_4$ (4.1 g, 4.40 mmol). Yield 4.22 g, 70%. $\text{C}_{72}\text{H}_{104}\text{V}_2\text{O}_8 \cdot 2\text{CH}_2\text{Cl}_2$ requires C 64.90, H, 7.95. Found C 64.82, H 8.02%. MS (solid, APCI): 1069.3 $[\text{M} - \text{O}t\text{Bu} - t\text{Bu}]^{2+}$. IR: 1570w, 1301w, 1261s, 1202w, 1189w, 1154w, 1091bs, 1018s, 915w, 880w, 862w, 799s, 722m, 661w, 645w. ^1H NMR (CDCl_3 , sample dried *in vacuo* for 12 h) δ : 7.33–7.13 ($3 \times$ m, 8H, arylH), 6.73 (s, 4H, arylH), 6.30 (s, 2H, CH), 5.29 (s, 4H, CH_2Cl_2), 1.69 (s, 18H, $\text{OC}(\text{CH}_3)_3$), 1.43 (s, 36H, $\text{C}(\text{CH}_3)_3$), 1.27 (s, 36H, $\text{C}(\text{CH}_3)_3$). ^{51}V NMR (CDCl_3) $\delta = -468.9$ ($w_{1/2} = 652$ Hz).



Synthesis of $\{[V(\text{NCMe})(\text{Np-MeC}_6\text{H}_4)\text{Cl}]_2(\mu\text{-}p\text{-L}^{\text{3P}})\} \cdot 5 \cdot 2\text{MeCN}$. $p\text{-L}^{\text{3P}}\text{H}_4$ (1.00 g, 1.08 mmol) and $[V(\text{Np-MeC}_6\text{H}_4)\text{Cl}_3]$ (0.60 g, 2.29 mmol) were stirred in THF (30 ml) for 5 min, then Et_3N (0.63 ml, 4.55 mmol) was added and the mixture was left to stir for 12 h. Following removal of volatiles *in vacuo*, the residue was extracted in MeCN (30 ml) and on prolonged standing (1–2 days) at ambient temperature, small prisms of **5** formed. Yield: 1.09 g, 69%. $\text{C}_{78}\text{H}_{100}\text{N}_2\text{Cl}_2\text{V}_2\text{O}_4$ (sample dried *in vacuo* for 12 h, -2MeCN) requires C, 71.92, H, 7.74, N, 2.15%. Found C 71.34, H 8.23, N 1.71%; despite repeated attempts, these were the best values we could obtain. MS (solid, APCI): 1302 $[\text{M} - 2\text{MeCN}]^+$, 1266 $[\text{M} - 2\text{MeCN} - \text{Cl}]^+$. IR: 2336w, 2309w, 2277w, 2251w, 1627w, 1586w, 1526w, 1504m, 1320m, 1320w, 1289m, 1260s, 1224m, 1200m, 1166w, 1106s, 1018s, 909w, 873w, 835m, 806s, 793m, 750w, 723w, 703w, 665m, 643w, 625w, 591m, 571w, 553w, 510w, 490s, 473w, 464w, 415m. ^1H NMR (CDCl_3): $\delta = 7.40\text{--}7.01$ (5 \times m, 20H, arylH + imidoarylH), 5.83 (s, 2H, CH), 2.22 (s, 6H, CH_3CN), 2.16 (s, 6H, $\text{CH}_3\text{C}_6\text{H}_4$), 1.59 (s, 36H, $\text{C}(\text{CH}_3)_3$), 1.29 (s, 36H, $\text{C}(\text{CH}_3)_3$); ^{51}V NMR (CDCl_3) $\delta = -218.9$ ($\omega_{1/2} = 1074$ Hz).

Ring opening polymerisation procedure

Polymerisation reactions were performed in a Schlenk tube equipped with a magnetic stirrer. For solution polymerisation, a mixture of monomer (14 mmol of ϵ -caprolactone, L-lactide or *rac*-lactide), vanadyl complexes **1–5** or **I** and **II** (0.14 mmol) and BnOH (0.14 mmol, if needed) were added into a Schlenk tube at room temperature under nitrogen protection. After 3 cycles of gassing and degassing, pre-degassed toluene (7 ml) was added to the reaction mixture under nitrogen protection. The polymerisation was started by placing the reaction mixture into an oil bath pre-heated to the polymerisation temperature (T_p). For bulk polymerisation, all reaction conditions were the same except that no solvent was used. In all cases, the polymerisation was stopped by addition of 1 ml methanol after the prescribed reaction time. Products with different polymerisation times were taken out with a syringe and precipitated into cold methanol with magnetic stirring to eliminate residual catalyst. Precipitates were filtrated, washed with methanol and dried before GPC determination.

Co-polymerisations were conducted by adding monomer 1 (3.200 mmol) to the catalyst (0.016 mmol) in toluene pre-heated to 80 °C and stirring for 24 h, and then adding monomer 2 (3.320 mmol) and stirring for a further 24 h. The polymerisation mixture was quenched by adding methanol (1.0 ml), and the resultant solution was then poured into methanol (200 ml), the precipitate collected and dried *in vacuo*.

Crystallography

Single crystal diffraction data were collected by the UK National Crystallography Service using a Rigaku FR-E+ diffractometer. This operates with a SuperBright rotating anode X-ray generator and high flux optics. This is designed to deal with the most challenging samples sent to the service.

Despite the high flux, the crystal of **1** examined was found to scatter X-rays very poorly and little appreciable diffraction was observed beyond ~ 1.1 Å. It was possible to solve the structure

using this data and routine refinements of a structural model were possible. It was possible to use anisotropic displacement parameters for all non-hydrogen atoms and the refinement was stable with no unusual features. Although the crystal examined was weakly scattering the solution is sound and it gives extremely useful chemical information.

The data for **2**, although weak, are more routine and standard procedures were applied in structure solution.

Structures were solved using Direct Methods implemented within SHELXS-2013 and refined within SHELXL-2014.²⁰

Further details are provided in Table S2.†

Acknowledgements

LJ thanks the National Natural Science Foundation of China (No. 50873067 and No. 51403140) and Research Fund for the Doctoral Program of Higher Education of China (No. 20110181110032 and International Scientific and Technological Cooperation Projects (No. 2010DFA54460) of China) for financial support. CR thanks the EPSRC for the award of a travel grant and Astatech Ltd (Chengdu) for loan of $[\text{VO}(\text{OnPr})_3]$ and di-phenol.

Notes and references

- For recent reviews see: (a) A. Corma, S. Iborra and A. Velty, *Chem. Rev.*, 2007, **107**, 2411; (b) C. K. Williams and M. A. Hillmyer, *Polym. Rev.*, 2008, **48**, 1; (c) E. S. Place, J. H. George, C. K. Williams and M. H. Stevens, *Coord. Chem. Rev.*, 2009, **38**, 1139.
- (a) M. Labet and W. Thielemans, *Chem. Soc. Rev.*, 2009, **38**, 3484; (b) A. Arbaoui and C. Redshaw, *Polym. Chem.*, 2010, **1**, 801; (c) X. Rong and C. Chunxia, *Progr. Chem.*, 2012, **24**, 1519.
- R. Mazarro, I. Gracia, J. F. Rodriguez, G. Storti and M. Morbidelli, *Polym. Int.*, 2012, **61**, 265.
- (a) C. Redshaw, *Dalton Trans.*, 2010, **39**, 5595; (b) K. Nomura and W. Zhang, *Chem. Rev.*, 2011, **111**, 2342; (c) J.-Q. Wu and Y.-S. Li, *Coord. Chem. Rev.*, 2011, **255**, 2303; (d) C. Redshaw, M. J. Walton, M. R. J. Elsegood, T. J. Prior and K. Michiue, *RSC Adv.*, 2015, **5**, 89783.
- C. Redshaw, M. R. J. Elsegood, J. A. Wright, H. Baillie-Johnson, T. Yamato, S. de Giovanni and A. Mueller, *Chem. Commun.*, 2012, **48**, 1129.
- (a) Y. Kim, P. N. Kapoor and J. G. Verkade, *Inorg. Chem.*, 2002, **41**, 4834; (b) C. Alonso-Moreno, A. Antiñolo, J. C. Garcia-Martinez, S. Garcia-Yuste, I. López-Solera, A. Otero, J. C. Perez-Flores and M. T. Tercero-Morales, *Eur. J. Inorg. Chem.*, 2012, 1139; (c) T. K. Saha, M. Mandel, M. Thunga, D. Chakraborty and V. Ramkumar, *Dalton Trans.*, 2012, **42**, 10304; (d) Y. Al-Khafaji, X. Sun, T. J. Prior, M. R. J. Elsegood and C. Redshaw, *Dalton Trans.*, 2015, **44**, 12349.
- Use of di-phenols: (a) B.-T. Ko and C.-C. Lin, *Macromolecules*, 1999, **32**, 8296; (b) I. Taden, H.-C. Kang, W. Massa, T. P. Spaniol and J. Okuda, *Eur. J. Inorg. Chem.*, 2000, 441; (c) H.-L. Chen, B.-T. Ko, B.-H. Huang and C.-C. Lin,



- Organometallics*, 2001, **20**, 5076; (d) B. T. Ko and C.-C. Lin, *J. Am. Chem. Soc.*, 2001, **123**, 7973; (e) Y.-C. Liu, B.-T. Ko and C.-C. Lin, *Macromolecules*, 2001, **34**, 6196; (f) M.-L. Hsueh, B.-H. Huang and C.-C. Lin, *Macromolecules*, 2002, **35**, 5763; (g) M. H. Chisholm, C.-C. Lin, J. C. Gallucci and B.-T. Ko, *Dalton Trans.*, 2003, 406; (h) T.-C. Liao, Y.-L. Huang, B.-H. Huang and C.-C. Lin, *Macromol. Chem. Phys.*, 2003, **204**, 885; (i) Y. Takashima, Y. Nakayama, T. Hirao, H. Yasuda and A. Harada, *J. Organomet. Chem.*, 2004, **689**, 612; (j) M.-L. Shueh, Y.-S. Wang, B.-H. Huang, C.-Y. Kuo and C.-C. Lin, *Macromolecules*, 2004, **37**, 5155; (k) R.-M. Ho, Y.-W. Chiang, C.-C. Tsai, C.-C. Lin, B.-T. Ko and B.-H. Huang, *J. Am. Chem. Soc.*, 2004, **126**, 2704; (l) T.-L. Yu, C.-C. Wu, C.-C. Chen, B.-H. Huang, J. Wu and C.-C. Lin, *Polymer*, 2005, **46**, 5909; (m) Y. Yao, X. Xu, B. Liu, Y. Zhang, Q. Shen and W.-T. Wong, *Inorg. Chem.*, 2005, **44**, 5133; (n) X. Xu, Z. Zhang, Y. Yao, Y. Zhang and Q. Shen, *Inorg. Chem.*, 2007, **46**, 9379; (o) M.-L. Hsueh, J. Wu and C.-C. Lin, *Macromolecules*, 2005, **38**, 9482; (p) J. Wu, Y.-Z. Chen, W.-C. Hung and C.-C. Lin, *Organometallics*, 2008, **27**, 4970; (q) Z. Liang, X. Ni, X. Li and Z. Shen, *Inorg. Chem. Commun.*, 2011, **14**, 1948; (r) C.-Y. Li, P.-S. Chen, S.-J. Hsu, C.-H. Lin, H.-Y. Huang and B.-T. Ko, *J. Organomet. Chem.*, 2012, **716**, 175; (s) X. Xu, X. Pan, S. Tang, X. Lv, L. Li, J. Wu and X. Zhao, *Inorg. Chem. Commun.*, 2013, **29**, 89; (t) Z. Liang, M. Zhang, X. Ni, X. Li and Z. Shen, *Inorg. Chem. Commun.*, 2013, **29**, 145.
- 8 Use of tetra-phenols: J. Zhang, C. Jian, Y. Gao, L. Wang, N. Tang and J. Wu, *Inorg. Chem.*, 2012, **51**, 13380.
- 9 (a) C. Redshaw, L. Warford, S. H. Dale and M. R. J. Elsegood, *Chem. Commun.*, 2004, 1954; (b) D. Homden, C. Redshaw, L. Warford, D. L. Hughes, J. A. Wright, S. H. Dale and M. R. J. Elsegood, *Dalton Trans.*, 2009, 8900.
- 10 P. J. Toscano, E. J. Schermerhorn, C. Dettelbacher, D. Macherone and J. Zubieta, *J. Chem. Soc., Chem. Commun.*, 1991, 933.
- 11 A. Arbaoui, D. Homden, C. Redshaw, J. A. Wright, S. H. Dale and M. R. J. Elsegood, *Dalton Trans.*, 2009, 8911.
- 12 T. Moriuchi, M. Nishina and T. Hirao, *Angew. Chem., Int. Ed.*, 2010, **49**, 83.
- 13 (a) A. L. Spek, *Acta Crystallogr.*, 1990, **A46**, C34; (b) P. V. D. Sluis and A. L. Spek, *Acta Crystallogr.*, 1990, **A46**, 194.
- 14 (a) W. Clegg, M. R. J. Elsegood, S. J. Teat, C. Redshaw and V. C. Gibson, *J. Chem. Soc., Dalton Trans.*, 1998, 3037; (b) W. Clegg, *J. Chem. Soc., Dalton Trans.*, 2000, 3223.
- 15 (a) E. A. Maatta, *Inorg. Chem.*, 1984, **23**, 2561–2562; (b) D. D. Devore, J. D. Lichtenhan, F. Takusagawa and E. A. Maatta, *J. Am. Chem. Soc.*, 1987, **109**, 7408.
- 16 See for example (a) Y. Takashima, Y. Nakayama, K. Watanabe, T. Itono, N. Ueyama, A. Nakamura, H. Yasuda, A. Harada and J. Okuda, *Macromolecules*, 2002, **35**, 7358; (b) Y. Kim, G. K. Jnaneshwara and J. G. Verkade, *Inorg. Chem.*, 2003, **42**, 1437.
- 17 A. Grala, J. Ejfler, L. B. Jerzykiewicz and P. Sobota, *Dalton Trans.*, 2011, **40**, 4042.
- 18 E. Piedra-Arroni, C. Ladavière, A. Amgoune and D. Bourissou, *J. Am. Chem. Soc.*, 2013, **135**, 13305.
- 19 S. Sriputtirat, W. Boonkong, S. Pengprecha, A. Petsom and N. Thongchul, *Adv. Chem. Eng. Sci.*, 2012, **2**, 15.
- 20 G. M. Sheldrick, *Acta Crystallogr.*, 2008, **64**, 112.

